Accepted by The Astrophysical Journal
Preprint typeset using LaTeX style emulateapj v. 11/10/09



# LONG-LIVED MAGNETIC-TENSION-DRIVEN MODES IN A MOLECULAR CLOUD

Shantanu Basu and Wolf B. Dapp
Department of Physics and Astronomy, University of Western Ontario, London, Ontario, N6A 3K7, Canada
*Accepted by The Astrophysical Journal*

## ABSTRACT

We calculate and analyze the longevity of magnetohydrodynamic (MHD) wave modes that occur in the plane of a magnetic thin sheet. Initial turbulent conditions applied to a magnetically subcritical cloud are shown to lead to relatively rapid energy decay if ambipolar diffusion is introduced at a level corresponding to partial ionization primarily by cosmic rays. However, in the flux-freezing limit, as may be applicable to photoionized molecular cloud envelopes, the turbulence persists at "nonlinear" levels in comparison with the isothermal sound speed $c_{\rm s}$, with one-dimensional rms material motions in the range of $\approx 2\,c_{\rm s} - 5\,c_{\rm s}$ for cloud sizes in the range of $\approx 2\,{\rm pc} - 16\,{\rm pc}$. These fluctuations persist indefinitely, maintaining a significant portion of the initial turbulent kinetic energy. We find the analytic explanation for these persistent fluctuations. They are magnetic-tension-driven modes associated with the interaction of the sheet with the external magnetic field. The phase speed of such modes is quite large, allowing residual motions to persist without dissipation in the flux-freezing limit, even as they are nonlinear with respect to the sound speed. We speculate that long-lived large-scale MHD modes such as these may provide the key to understanding observed supersonic motions in molecular clouds.

*Subject headings:* instabilities — ISM: clouds — ISM: magnetic fields — magnetohydrodynamics (MHD) — stars: formation

## 1. INTRODUCTION

Nonthermal linewidths are ubiquitous in molecular clouds (Solomon et al. 1987) and are interpreted to represent highly supersonic random internal motions (see McKee & Ostriker 2007, for a recent review). Principal component analysis (Brunt et al. 2009) reveals that most of the energy is contained in modes that span the largest scale of the cloud.

Since molecular clouds are threaded by large-scale magnetic fields, an attractive suggestion has been that the turbulence represents supersonic but sub-Alfvénic magnetohydrodynamic (MHD) waves, with the noncompressive shear Alfvén mode identified as a possible long-lived component (Arons & Max 1975). This was intended to bypass the usual problem of rapid dissipation of supersonic hydrodynamic turbulence through shocks. A compilation of available Zeeman measurements of the (line-of-sight) magnetic field strength, gas density $\rho$, and one-dimensional velocity dispersion $\sigma_v$ shows that cloud fragments obey a direct linear correlation between $\sigma_v$ and the mean Alfvén speed $V_{\rm A}$ (Myers & Goodman 1988; Basu 2000), with a proportionality coefficient $\approx 0.5$. This correlation may be attributed to a rough equality of the magnitudes of gravitational, magnetic, and turbulent energies, and was interpreted by Mouschovias & Psaltis (1995) and Mouschovias et al. (2006) to mean that the motions are Alfvénic disturbances in which the perturbed magnetic field is comparable in strength to the background magnetic field. Furthermore, the MHD motions in a molecular cloud may represent long-wavelength standing waves, as argued by Mouschovias (1975, 1987). This brings out the possibility of "global" effects (e.g. due to cloud boundaries and external interaction) being important in understanding cloud turbulence, and the need to go beyond comparing observations with models of wave propagation in an infinite medium.

In direct contrast to the scenario of long-lived motions, numerical simulations of molecular cloud turbulence using a three-dimensional simulation cube with periodic boundary conditions have revealed that supersonic MHD turbulence decays away rapidly, like its hydrodynamic counterpart, on about a sound crossing time of the driving scale (Stone et al. 1998; Mac Low et al. 1998; Mac Low 1999; Ostriker et al. 2001). This happens in either the case of sub-Alfvénic or super-Alfvénic turbulence, and in both cases, turbulence is maintained for long periods only by constant driving of velocity perturbations in Fourier space. When interpreting the above results, we should keep in mind that periodic box simulations represent a "local" patch of uniform background density that is embedded within a larger cloud, and are equivalent to studying an infinite uniform medium. By comparison, a 1.5-dimensional global model including vertical stratification (Kudoh & Basu 2003, 2006) found that the decay of turbulence could be delayed, but only mildly, by some transfer of internal kinetic energy from small to large scale modes along the magnetic field direction. The rapid turbulence dissipation in all of these models is due to the presence of shocks and takes place under the assumption of magnetic flux freezing, without any contribution from magnetic field dissipation, e.g., by ambipolar diffusion.

The bottom line from the above studies is that all previous numerical modeling of MHD turbulence leads to rapid dissipation, in about a crossing time, with a logical conclusion that matching observations requires vigorous driving of turbulence from unspecified sources. The alternate possibility of maintaining some long-lived global modes is appealing but remained largely unex-

basu@uwo.ca
wdapp@uwo.ca

plored quantitatively.

In a recent paper, Basu et al. (2009b) carried out an extensive parameter survey of fragmentation initiated by nonlinear turbulent flows, employing the magnetic thin-sheet approximation and also including the effect of ambipolar diffusion (see also Basu & Ciolek 2004; Li & Nakamura 2004; Nakamura & Li 2005; Ciolek & Basu 2006; Basu et al. 2009a). In this approximation, the sheet interacts at its upper and lower surfaces with an external magnetic field, and can be considered a global model in the $z$-direction (parallel to the mean background magnetic field), although it is a local (periodic) model in the $x$- and $y$-directions. Basu et al. (2009b) found that initial turbulent fluctuations decayed away quite rapidly in all models with supercritical mass-to-flux ratio, as well as for subcritical models that included the effect of ambipolar diffusion. However, a surprising result was that subcritical clouds evolving under flux-freezing were able to maintain a substantial portion of their initial kinetic energy to indefinitely large times.

In this paper, we analyze this unique instance of a turbulent MHD simulation that yields long-lived nonlinear motions. We perform a suite of numerical simulations to test its generality, and also establish an analytic explanation for this very interesting result.

## 2. METHOD

The thin-sheet equations are obtained by vertically integrating the full equations for a partially ionized, magnetic, self-gravitating, isothermal fluid in the vertical direction from $z = -Z(x, y)$ to $z = +Z(x, y)$. Details of this integration are found in Ciolek & Mouschovias (1993) and Ciolek & Basu (2006). The nonaxisymmetric thin-sheet equations, formulation of our model, and our numerical methods are described in several papers (Ciolek & Basu 2006; Basu et al. 2009a,b). The evolution equations for the magnetized thin sheet include the effects of magnetic tension due to the external magnetic field $\boldsymbol{B}(x, y, z)$. It is calculated as a potential field, with the vertical magnetic field in the equatorial plane, $B_{z,\rm eq}(x, y)$, acting as a source for $\boldsymbol{B}(x, y, z) - B_{\rm ref}\hat{z}$, much as $\sigma_{\rm n}(x, y)$ acts as a source for the gravitational field. Periodic boundary conditions are applied to a square Cartesian region of size $L$. The initial background state has a uniform (in the $x$- and $y$- directions) neutral surface density $\sigma_{\rm n,0}$ and a uniform vertical ($z$-direction) magnetic field $B_{\rm ref}$. We input nonlinear velocity fluctuations with spectrum $v_k^2 \propto k^{-4}$ in Fourier space, where $k$ is the absolute value of the wavenumber, and modes are damped at a fixed (small) scale that is independent of the box size or the number of grid zones used in a simulation.

The gas is isothermal with sound speed $c_{\rm s}$, and partial ionization is mainly due to cosmic rays. This introduces the dimensionless free parameter $\tilde{\tau}_{\rm ni,0} \equiv \tau_{\rm ni,0}/t_0$, where $\tau_{\rm ni,0}$ is the initial neutral-ion collision time, and $t_0 = c_{\rm s}/2\pi G\sigma_{\rm n,0}$ is a characteristic time in the problem. The flux-freezing limit, used extensively in this paper, corresponds to $\tilde{\tau}_{\rm ni,0} = 0$. Another important parameter is the initial dimensionless mass-to-flux ratio $\mu_0 \equiv 2\pi G^{1/2}\sigma_{\rm n,0}/B_{\rm ref}$, i.e., $\mu_0 > 1$ yields a supercritical cloud in which fragmentation occurs dynamically and $\mu_0 < 1$ yields a subcritical cloud in which fragmentation is driven on a longer time scale by ambipolar diffusion (see Ciolek & Basu 2006). Turbulent initial conditions introduce the dimensionless parameter $v_a/c_{\rm s}$, where $v_a$ is the rms amplitude of the initial velocity fluctuations in each direction. Finally, we also vary the ratio $L/L_0$ (where $L_0 = c_{\rm s}^2/2\pi G\sigma_{\rm n,0}$ is a characteristic length scale of the system), and $N$, the number of grid zones in each direction. An additional parameter, the dimensionless external pressure $\tilde{P}_{\rm ext} = 2P_{\rm ext}/\pi G\sigma_{\rm n,0}^2$, is kept fixed at 0.1 in all models, and does not play an important role in the dynamics.

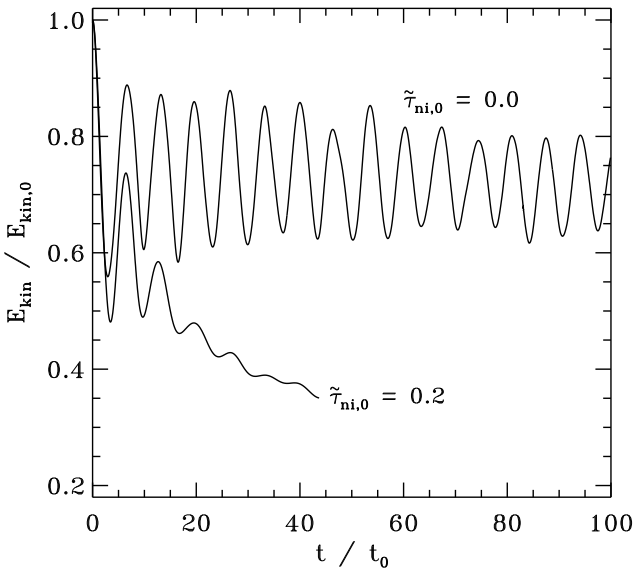


FIG. 1.— Kinetic energy $E_{\rm kin}$ normalized to its initial value $E_{\rm kin,0}$ for two models. Each model has $\mu_0 = 0.5$, $v_a = 2c_{\rm s}$, and $L/L_0 = 32\pi$. One model evolves with flux freezing, $\tilde{\tau}_{\rm ni,0} = 0$, and is run with $N = 512$. The other model has partial coupling of neutrals and ions characterized by $\tilde{\tau}_{\rm ni,0} = 0.2$, and is run with $N = 1024$.

## 3. RESULTS

### 3.1. *Canonical models*

Two models illustrate the key result for subcritical clouds with turbulent initial conditions. Figure 1 shows the time evolution of total kinetic energy for a model which allows for neutral-ion drift ($\tilde{\tau}_{\rm ni,0} = 0.2$), and another model which has flux freezing ($\tilde{\tau}_{\rm ni,0} = 0$). The value $\tilde{\tau}_{\rm ni,0} = 0.2$ corresponds to the canonical ionization fraction implied by primarily cosmic ray ionization: $\chi_{\rm i} \simeq 10^{-7}(n_{\rm n}/10^4\ {\rm cm}^{-3})^{-1/2}$ (see Tielens 2005), where $n_{\rm n}$ is the number density of neutrals. Both models are characterized by $\mu_0 = 0.5, v_a = 2\,c_{\rm s}, L = 32\pi L_0$. The flux-frozen run has $N = 512$ while the ambipolar diffusion run has $N = 1024$. The evolution of the ambipolar diffusion model terminates at time $t = 45.4\,t_0$, when the highest column density in the simulation reaches $100\,\sigma_{\rm n,0}$ — a useful proxy for runaway collapse of the first core. At this time, the kinetic energy has decayed away substantially, and appears to still be declining. In contrast, the flux-frozen model has, after an initial loss of some kinetic energy, stabilized to executing oscillations about a mean value $E_{\rm kin} \approx 0.7\,E_{\rm kin,0}$. We have run simulations with flux freezing up to $t \approx 35,000\,t_0$ with no change in this behavior.

Figure 2 shows color images of the column density for

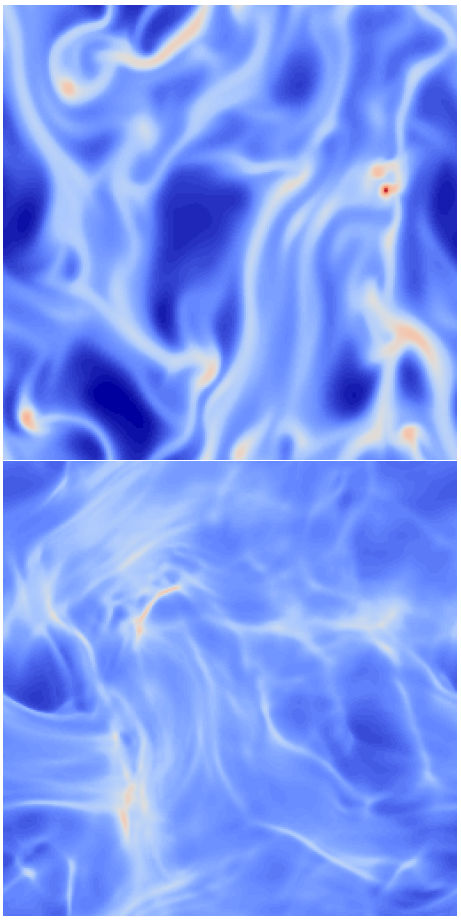

FIG. 2.— Images of gas column density $\sigma_{\rm n}(x,y)/\sigma_{\rm n,0}$ for models with ambipolar diffusion (top) and flux freezing (bottom), shown in identical color schemes that are proportional to the logarithm of the column density. Both models have $\mu_0 = 0.5$, initial turbulence with $v_a = 2\,c_{\rm s}$ and spectrum $v_k^2 \propto k^{-4}$, and are run with $N = 256$. The ambipolar diffusion model terminates at time $t = 43.5\,t_0$ in this realization due to the eventual runaway collapse of a core (in the upper right of the image). The flux-frozen model is shown at the same time, but continues to evolve to indefinitely large times without collapse. It shows a more wispy column density structure, with no evidence of monolithic collapse toward any density peaks. An animation of the evolution of each model is available online.

models that are equivalent to the ones described above, but with $N = 256$. The ambipolar diffusion model is shown at its end time $t = 43.5\,t_0$, and the flux-frozen model is shown at the same time, although it continues to evolve indefinitely. The ambipolar diffusion model shows evidence of monolithic collapse toward one or more density peaks, while the flux-frozen model shows a more wispy character and gives no indication of impending collapse in any region, neither visually nor quantitatively. Figure 3 shows a model snapshot of the flux-frozen model but viewed from a three-dimensional perspective, with the external field lines illustrated in the region above the sheet. Since this is a subcritical model, the field lines are not significantly deformed. The pitch angle of the magnetic field relative to the vertical direction, measured at the sheet surface, maintains an average value that is a little less than 10°. For a comparison of field line curvature for models with a range of $\mu_0$, see Basu et al. (2009a,b). Animations of both Figures 2 and 3, with the latter also showing external field line evolution, are available online.

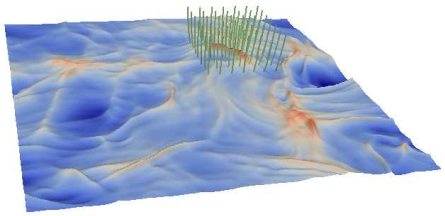

FIG. 3.— Surface map of gas column density $\sigma_{\rm n}(x,y)/\sigma_{\rm n,0}$ for the same flux-frozen model that is shown in Fig. 2. The elevation and color of the surface is proportional to the logarithm of the local column density. The sheet is viewed from a non-face-on viewing angle. The external magnetic field above the sheet is also represented by field lines, in a region near a density peak. An animation of the evolution of the model, including field line evolution, is available online.

### 3.2. *Connection to Linear Analysis*

To gain insight into the long-lived mode for the flux-freezing model, we revisit the modal analysis of a partially ionized magnetized sheet. This has been carried out by Morton (1991) and Ciolek & Basu (2006). Starting with a static uniform background, the thin-sheet equations can be expanded by writing any physical quantity $f(x,y,t) = f_0 + \delta f_a \exp[i(k_x x + k_y y - \omega t)]$, where $f_0$ is the unperturbed state, $\delta f_a$ is the amplitude of the perturbation, $k_x$ and $k_y$ are the wavenumbers in the $x$- and $y$- directions, and $\omega$ is a complex angular frequency. For assumed small perturbations, one can retain only terms up to first order in perturbed quantities, resulting in Equations 32(a) - 32(d) of Ciolek & Basu (2006). Those equations can be combined to yield the dispersion relation

$$(\omega + i\,\theta)\left[\omega^2 - C_{\rm eff}^2 k^2 + 2\pi G\sigma_{\rm n,0} k\right] = \omega\left[V_{\rm A,0}^2 k^2 + 2\pi G\sigma_{\rm n,0}\,\mu_0^{-2} k\right], \quad (1)$$

where

$$\theta = 2\pi\,\tau_{\rm ni,0}\left[V_{\rm A,0}^2 k^2 + 2\pi G\sigma_{\rm n,0}\,\mu_0^{-2} k\right] \quad (2)$$

contains the effect of ambipolar diffusion. In the above equations, we have introduced the Alfvén speed $V_{\rm A,0}$ for physical clarity of the magnetic-pressure-driven terms proportional to $k^2$ ($\equiv k_x^2 + k_y^2$), while retaining $\mu_0$ for physical clarity of the magnetic-tension-driven terms proportional to $k$ ($\equiv |\sqrt{k^2}|$). The two parameters are actually related: $V_{\rm A,0}^2 \equiv B_{\rm ref}^2/4\pi\rho_{\rm n,0} = 2\pi G\sigma_{\rm n,0}\mu_0^{-2} Z_0$, where the sheet half-thickness $Z_0 = \sigma_{\rm n,0}/2\rho_{\rm n,0}$ and $\rho_{\rm n,0}$ is its mass volume density. The quantity $C_{\rm eff}$ is an effective sound speed that takes into account the restoring force due to an external pressure $P_{\rm ext}$ (see Ciolek & Basu 2006). In the flux-freezing limit, Equation (1) becomes

$$\omega^2 = (V_{\rm A,0}^2 + C_{\rm eff}^2)\,k^2 + 2\pi G\sigma_{\rm n,0}\,(\mu_0^{-2} - 1)k. \quad (3)$$

In the case of subcritical clouds ($\mu_0 < 1$), the second term on the right-hand side becomes a stabilizing term rather than a destabilizing term associated with gravitational instability. However, the full dispersion relation (Equation (1)) does contain destabilizing terms due to ambipolar diffusion; the effect on a subcritical cloud is a "slow" instability leading to collapse on an ambipolar diffusion time scale rather than a dynamical time. Equation (42) of Ciolek & Basu (2006) yields a good approximation to the ambipolar diffusion growth time for significantly subcritical clouds.

Equation (3) shows that long-wavelength modes evolving under flux freezing have a phase speed

$$V_{\rm MT,0} \equiv \frac{\omega}{k} = \sqrt{(\mu_0^{-2} - 1) G \sigma_{\rm n,0} \lambda}\,, \qquad (4)$$

where $\lambda = 2\pi/k$. These modes are driven by the restoring force of the magnetic tension of inclined field lines that connect the sheet to the external medium. These magnetic-tension-driven modes should not be confused with the traditional MHD wave modes. Within the thin sheet, in the short-wavelength limit, magnetic pressure drives the magnetosound mode with phase speed $V_{\rm MS,0} = (V_{\rm A,0}^2 + C_{\rm eff}^2)^{1/2}$.

Since $V_{\rm MT,0} \propto \sqrt{\lambda}$, it achieves significant values (much larger than $V_{\rm MS,0}$), for $\mu_0 = 0.5$ and wavelengths equal to the box sizes we consider: $L = 16\pi\, L_0 - 128\pi\, L_0$. The values are in the range $4.9\, c_{\rm s} - 13.9\, c_{\rm s}$ and typical values of input parameters would correspond to dimensional box sizes $\approx 2 - 16$ pc (see Basu et al. 2009a,b, for scaling of units). Since the restoring force is provided by the external potential field that can adjust instantaneously as the sheet evolves, the modes found in this linear analysis cannot be applied to arbitrarily large wavelengths. In reality, there must be time for readjustment of the external field. The magnetic potential $\Psi_M(x, y, z)$ above and below the sheet decays as $\exp(-k|z|)$ (see Ciolek & Basu 2006; Basu et al. 2009a), so that a characteristic height of deformation of the field lines is $k^{-1}$. The ratio $\epsilon$ of the Alfvén crossing time across this distance divided by the wave period must be well below unity in order for the potential field approximation to be valid. While the Alfvén crossing time grows more rapidly ($\propto \lambda$) with increasing wavelength than does the wave period ($\propto \sqrt{\lambda}$), we find that $\epsilon \leq 0.26$ for modes of even our largest box size, if the external density $\rho_{\rm ext} \leq 0.1\, \rho_{\rm n,0}$. The nature of a low-density medium external to clouds or clumps is discussed in Section 4.

An interesting analogy can be made between the magnetic-tension-driven modes and gravity-driven waves in deep water. There, the undulations of wavenumber $k$ on a water surface can be felt down to a characteristic depth $k^{-1}$. Velocities below the surface are determined from a velocity potential solution of Laplace's equation. This is partly due to the incompressible fluid approximation in which the water pressure can adjust instantaneously. A clearer mathematical analogy also occurs in the following manner. Since the vertical gravitational field above and below a uniform thin sheet has magnitude $|g_z| = 2\pi G \sigma_{\rm n,0}$, Equation (4) may be rewritten as

$$V_{\rm MT,0} = \sqrt{(\mu_0^{-2} - 1)|g_z|/k}\,, \qquad (5)$$

in analogy to the phase speed $v = \sqrt{g/k}$ for deep water waves in a constant gravitational field $g$.

### 3.3. *Further modeling*

The implication of the high values of $V_{\rm MT,0}$ for the magnetic-tension-driven modes in the plane of a thin sheet is that waves with nonlinear particle motions (in comparison to the sound speed $c_{\rm s}$ or magnetosound speed $V_{\rm MS,0}$) may still act as linear waves since their material motions are much slower than $V_{\rm MT,0}$. They will then evolve (in the flux-freezing limit) without any nonlinear distortion and dissipation. All models do lose significant kinetic energy in an early phase, due to shocks and compression that leads to significant losses in an isothermal gas. Small-scale modes are prone to such decay; for them the relevant signal speed is $V_{\rm MS,0}$, which equals $2.9\, c_{\rm s}$ for the models presented in Section 3.1. However, the $v_k^2 \propto k^{-4}$ spectrum means that most of the energy is in the largest scale mode, which can survive indefinitely, as long as the velocity amplitude is significantly less than $V_{\rm MT,0}$, either initially or after some nonlinear decay. In the magnetic-tension-driven mode, energy is stored and released by the magnetic field, without losses due to ambipolar diffusion (in the $\tilde{\tau}_{\rm ni,0} = 0$ models) or other forms of magnetic field dissipation. Furthermore, the isothermal assumption does not rob any net energy at this stage. In symmetric oscillations, energy is lost during wave compressions and an equal amount gained back during wave expansions.

Figure 4 explores the effect of different initial conditions on the decay and residual amount of turbulence in several flux-frozen ($\tilde{\tau}_{\rm ni,0} = 0$) models. The top panel shows a comparison of models with $v_k^2$ proportional to $k^{-4}$, $k^{-2}$, and $k^0$, respectively, but all having the same initial rms speed. The spectrum with the greatest amount of energy on the largest scale retains the most energy, as it is the largest scale mode that has the greatest phase speed and is most likely to survive with significant amplitude. The bottom panel shows that models with fixed spectrum $v_k^2 \propto k^{-4}$ but differing $v_a$ will lose different proportions of their initial turbulent energy. The phase speed of the largest mode in these simulation boxes is $V_{\rm MT,0} = 4.9\, c_{\rm s}$, and increasing $v_a$ leads to greater proportionate loss of initial kinetic energy. However, there is a weak trend toward retaining a greater *absolute* amount of energy, as a tabulation of $v_{\rm rms}$, the one-dimensional rms speed at $t \approx 100\, t_0$ in each simulation, reveals. Table 1 lists $v_{\rm rms}$ for many models that have flux-freezing, $\mu_0 = 0.5$, and $v_k^2 \propto k^{-4}$ initially. Supersonic motions remain in all models, and the residual amplitude rises with increasing box size as well as initial velocity amplitude $v_a$. The values of $v_{\rm rms}$ appear to saturate however, so that they remain a reasonably small fraction (14%-56%) of $V_{\rm MT,0}$ for each model.

Oscillations of the kinetic energy are clearly visible in the models that retain a large part of their initial energy, so that the values of $v_{\rm rms}$ in Table 1 are varying by up to 10%. The dominance of the largest mode in the initial conditions and the preferential nonlinear damping of smaller modes implies that the period of the largest mode is a reasonable approximation to these observed periods $P$. We determine $P$ by an average over many peak-to-peak oscillations in each model. The kinetic energy should oscillate with half the period of the velocity eigenfunction, so its expected period is

$$P = \frac{1}{2}\frac{L}{V_{\rm MT,0}} = \frac{1}{2}\left[\frac{L}{(\mu_0^{-2} - 1) G \sigma_{\rm n,0}}\right]^{1/2}, \qquad (6)$$

where we have used $\lambda = L$. In terms of the dimensionless box size $L/L_0$ and $t_0$, we can write this as

$$P = \frac{1}{2}\left[\frac{2\pi (L/L_0)}{\mu_0^{-2} - 1}\right]^{1/2} t_0\,. \qquad (7)$$

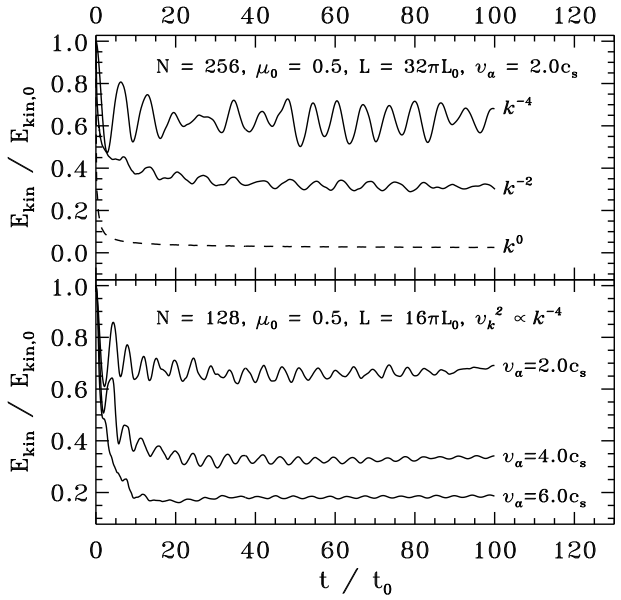


FIG. 4.— Effect of different power spectra and turbulent velocity amplitudes on kinetic energy decay. All models evolve with flux freezing ($\tilde{\tau}_{\rm ni,0} = 0$). Top panel: three models with fixed $v_a$ and other parameters (as labeled) but differing power spectra of initial turbulence, as labeled next to each curve. The model with the most energy on the largest scale retains the greatest part of its energy. Bottom panel: three models with differing $v_a$ but all other parameters including the power spectrum kept fixed, as labeled. Models with greater $v_a$ lose a greater proportion of their initial kinetic energy, although they retain a slightly greater absolute amount of kinetic energy (see Table 1).

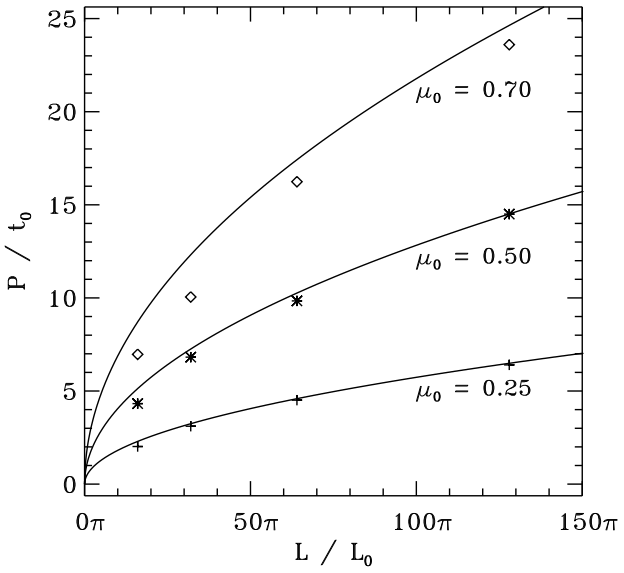


FIG. 5.— Comparison of analytically predicted periods of kinetic energy oscillation with results of simulations. Solid lines are the predicted periods from the linear theory of large-scale flux-frozen modes driven by magnetic tension, for three different values of the dimensionless mass-to-flux ratio $\mu_0 = (0.25, 0.5, 0.7)$. Open diamonds represent average periods of oscillation for four models of differing box size $L$ and fixed $\mu_0 = 0.7$. Asterisks and plus signs represent the same but for fixed $\mu_0 = 0.5$ and $\mu_0 = 0.25$, respectively. The agreement is between the solid lines and symbols is remarkably good, and best for the largest box sizes, since the analytic prediction is made in the long-wavelength limit.

TABLE 1
VELOCITY AMPLITUDE RESULTS FOR SELECTED MODELS

| $N$ | $L/L_0$ | $V_{\rm MT,0}/c_{\rm s}$ | $v_a/c_{\rm s}$ | $v_{\rm rms}/c_{\rm s}$ | $v_{\rm rms}/V_{\rm MT,0}$ |
|---|---|---|---|---|---|
| 128 | $16\pi$ | 4.9 | 2 | 1.7 | 0.35 |
| 128 | $16\pi$ | 4.9 | 4 | 2.4 | 0.48 |
| 128 | $16\pi$ | 4.9 | 6 | 2.6 | 0.53 |
| 256 | $32\pi$ | 6.9 | 2 | 1.6 | 0.23 |
| 256 | $32\pi$ | 6.9 | 4 | 3.4 | 0.49 |
| 256 | $32\pi$ | 6.9 | 6 | 3.9 | 0.56 |
| 512 | $32\pi$ | 6.9 | 2 | 1.7 | 0.25 |
| 512 | $64\pi$ | 9.8 | 2 | 1.9 | 0.19 |
| 512 | $64\pi$ | 9.8 | 3 | 2.7 | 0.28 |
| 512 | $64\pi$ | 9.8 | 4 | 2.9 | 0.29 |
| 1024 | $128\pi$ | 13.9 | 2 | 1.9 | 0.14 |
| 1024 | $128\pi$ | 13.9 | 4 | 3.4 | 0.25 |
| 1024 | $128\pi$ | 13.9 | 6 | 5.0 | 0.36 |

NOTE. — All models above have $\mu_0 = 0.5$, $\tilde{\tau}_{\rm ni,0} = 0$, and initial turbulent spectrum $v_k^2 \propto k^{-4}$. The one-dimensional velocity dispersion $v_{\rm rms}$ is measured at $t \approx 100\,t_0$ and is present indefinitely with variability of up to 10%.

Figure 5 shows the predicted dependence in solid lines, for $\mu_0 = (0.25, 0.5, 0.7)$. Different symbols as described in the figure caption represent the empirical determinations of $P$ from various models. The agreement is remarkably good, and improves for the largest box sizes, where the long-wavelength approximation made in Equation (4) holds particularly well.

## 4. DISCUSSION

The study of the decay of MHD turbulence has generally been based on the modeling of Alfvén, slow MHD, and fast MHD modes in media that have a uniform background. The study of more complex global MHD (including magnetogravitational) modes for molecular clouds remains to be explored. In this paper, we have analyzed turbulent decay in a magnetically subcritical sheet-like cloud. It is an idealized model of a molecular cloud that is tied to a magnetic field anchored in the interstellar medium. A large fraction of the initial input kinetic energy is retained by the deformed magnetic field, and then persists in the cloud as large-scale oscillations. These represent linear waves of large extent which are nevertheless supersonic since the phase speed of the magnetic-tension-driven modes is up to $\approx 10$ times the sound speed for typical cloud sizes.

Our model may approximate the situation of molecular clouds that are embedded in a low-density warm H I halo, or even the case of molecular cloud clumps that may be embedded in a matrix of H I gas (see Hennebelle & Inutsuka 2006). Flux freezing is a good approximation for molecular cloud envelopes (as opposed to dense cores), due to significant photoionization by background starlight (McKee 1989; Ciolek & Mouschovias 1995). Observations also reveal that the low-column-density molecular cloud envelopes actually contain most of the cloud mass (Kirk et al. 2006; Goldsmith et al. 2008). These envelopes may have a subcritical mass-to-flux ratio, as implied by their lack of star formation (Kirk et al. 2006), velocity data (e.g., in Taurus, Heyer et al. 2008), and the subcritical state of the H I clouds (Heiles & Troland 2005) from which molecular clouds are presumably assembled.

Continuous driving of turbulent motions in molecular clouds is often invoked because the canonical numerical result of decay in a crossing time (e.g., Stone et al. 1998; Mac Low 1999) is inconsistent with estimated cloud lifetimes that are at least a few crossing times (Williams & McKee 1997). Basu & Murali (2001) have argued that continuous driving of turbulence is consistent with observational constraints only if the driving occurs on the largest scale in the cloud, i.e., most of the energy is contained on that scale. Furthermore, continuous driving may not even be required if the decay time of the large-scale modes is greater than or equal to the estimated cloud lifetimes. Our models suggest that large-scale modes that are coupled to the external magnetic field can persist for very long times, thus reducing the need for continuous driving in order to explain observations. These modes preferentially span the largest scales in the model cloud, in agreement with analysis of observed cloud turbulence (Brunt et al. 2009). Future spectral line modeling of the large-scale cloud oscillations in our model cloud may make for useful comparison with observations, as has been done in a previous study of motions in the vicinity of dense cores (Kirk et al. 2009).

A counter-effect to the maintenance of large-scale modes is the loss of energy to the external medium. This can be accomplished by a coupling of the magnetic-tension-driven modes to MHD modes in the external medium. In a related example, Eng (2002) found significant energy loss to an external medium during core contraction using an approximate treatment of the transmission of transverse Alfvén waves through the bounding surfaces of a thin sheet. Some form of MHD wave coupling is certainly at work between any molecular cloud and its environment, although one may also argue that a clump embedded in a larger complex may reach a steady state in which it gains as much energy from its exterior as it loses. In any case, the study of the propagation of waves outside the cloud is outside the scope of our model. Future three-dimensional global MHD models of molecular clouds, which include the effect of an external medium, can address this point.

## 5. SUMMARY

We have demonstrated that MHD modes driven by the tension of inclined magnetic field lines have a large phase speed for subcritical clouds, which increases in proportion to the square root of the wavelength. Numerical simulations show that nonlinear motions (in comparison to the sound speed) persist indefinitely for thin-sheet evolution in the limit of magnetic flux-freezing. These are the first of any variety of MHD turbulence simulations that show long-lived nonlinear motions. For the broad set of models that we study, the residual one-dimensional rms material motions are in the range of $\approx 2\,c_{\rm s} - 5\,c_{\rm s}$ for cloud sizes in the range of $\approx 2\,{\rm pc} - 16\,{\rm pc}$. We find that runaway collapse toward isolated density peaks occurs when partial ionization due to (primarily) cosmic rays and ambipolar diffusion is included. However, the flux-freezing results can be relevant to understanding the low-column-density molecular cloud envelopes, which are photoionized to the level of effective flux-freezing, and contain most of the mass in a molecular cloud. For those regions, there is a particularly important role for wave modes driven by a magnetic field that threads the cloud and is connected to an external medium. Long-wavelength modes such as the ones we study may provide at least part of the explanation for widely observed supersonic motions in molecular clouds.

We thank the referee for insightful comments. S.B. acknowledges the hospitality of the Isaac Newton Institute for Mathematical Sciences at Cambridge University during the writing of this paper. S.B. was supported by a Discovery Grant from NSERC. W.B.D was supported by an Alexander Graham Bell Canada Graduate Scholarship from NSERC.

## REFERENCES

Arons, J., & Max, C. E. 1975, ApJ, 196, L77
Basu, S. 2000, ApJ, 540, L103
Basu, S., & Ciolek, G. E. 2004, ApJ, 607, L39
Basu, S., Ciolek, G. E., Dapp, W. B., & Wurster, J. 2009b, New Astron., 14, 483
Basu, S., Ciolek, G. E., & Wurster, J. 2009a, New Astron., 14, 221
Basu, S., & Murali, C. 2001, ApJ, 551, 743
Brunt, C. M., Heyer, M. H., & Mac Low, M.-M. 2009, A&A, 504, 883
Ciolek, G. E., & Basu, S. 2006, ApJ, 652, 442
Ciolek, G. E., & Mouschovias, T. Ch. 1993, ApJ, 418, 774
Ciolek, G. E., & Mouschovias, T. Ch. 1995, ApJ, 454, 194
Eng, C. 2002, PhD Thesis, Univ. of Illinois, Urbana-Champaign
Goldsmith, P. F., Heyer, M., Narayanan, G., Snell, R., Li, D., & Brunt, C. 2008, ApJ, 680, 428
Heiles, C., & Troland, T. H. 2005, ApJ, 624, 773
Hennebelle, P., & Inutsuka, S.-i. 2006, ApJ, 647, 404
Heyer, M., Gong, H., Ostriker, E., Brunt, C. 2008, ApJ, 680, 420
Kirk, H., Johnstone, D., & Basu, S. 2009, ApJ, 699, 1433
Kirk, H., Johnstone, D., & Di Francesco, J. 2006, ApJ, 646, 1009
Kudoh, T., & Basu. S. 2003, ApJ, 595, 842
Kudoh, T., & Basu. S. 2006, ApJ, 642, 270
Li, Z.-Y., & Nakamura, F. 2004, ApJ, 609, L83
Mac Low, M.-M. 1999, ApJ, 524, 169
Mac Low, M.-M., Klessen, R. S., Burkert, A., & Smith, M. D. 1998, Phys. Rev. Lett. 80, 2754
McKee, C. F. 1989, ApJ, 345, 782
McKee, C. F., & Ostriker, E. C. 2007, ARA&A, 45, 565
Morton, S. A. 1991, PhD Thesis, Univ. of Illinois, Urbana-Champaign
Mouschovias, T. Ch. 1975, PhD Thesis, Univ. of California, Berkeley
Mouschovias, T. Ch. 1987, in Physical Processes in Interstellar Clouds, ed. G. Morfil & M. Scholer (Dordrecht: Springer), 453
Mouschovias, T. Ch., Tassis, K., & Kunz, M. W. 2006, ApJ, 646, 1043
Mouschovias, T. Ch., & Psaltis, D. 1995, ApJ, 444, L105
Myers, P. C., & Goodman, A. A. 1988, ApJ, 326 L27
Nakamura, F., & Li, Z.-Y. 2005, ApJ, 631, 411
Ostriker, E. C., Stone, J. M., & Gammie, C. F. 2001, ApJ, 546, 980
Solomon, P. M., Rivolo, A. R., Barrett, J., & Yahil, A. 1987, ApJ, 319, 730
Stone, J. M., Gammie, C. F., & Ostriker, E. C. 1998, ApJ, 508, L99
Tielens, A. G. G. M. 2005, The Physics and Chemistry of the Interstellar Medium, (Cambridge: Cambridge Univ. Press)
Williams, J. P., & McKee, C. F. 1997, ApJ, 476, 166